Am J Cancer Res 2020;10(2):572-580
www.ajcr.us /ISSN:2156-6976/ajcr0103999

Original Article

Establishment of patient-derived tumor xenograft models of mucinous ovarian cancer

Francesca Ricci[1], Federica Guffanti[1], Roberta Affatato[1], Laura Brunelli[4], Pastorelli Roberta[4], Robert Fruscio[5], Patrizia Perego[6], Maria Rosa Bani[2], Giovanna Chiorino[7], Andrea Rinaldi[8], Francesco Bertoni[8], Maddalena Fratelli[3], Giovanna Damia[1]

[1]Laboratory of Molecular Pharmacology, [2]Laboratory of Laboratory of Biology and Treatment of Metastasis, [3]Laboratory of Molecular Biology, Istituto di Ricerche Farmacologiche Mario Negri IRCCS, Milan 20156, Italy; [4]Protein and Gene Biomarkers Unit, Laboratory of Mass Spectrometry, Department of Environmental Health Sciences, Istituto di Ricerche Farmacologiche Mario Negri IRCCS, Milan 20156, Italy; [5]Clinic of Obstetrics and Gynecology, Department of Medicine and Surgery, San Gerardo Hospital, University of Milan Bicocca, Monza 20900, Italy; [6]Clinic of Obstetrics and Gynecology, San Gerardo Hospital, Monza 20900, Italy; [7]Cancer Genomics Laboratory, Fondazione Edo and Elvo Tempia, Biella, Italy; [8]Institute of Oncology Research, Università della Svizzera italiana, Bellinzona 6500, Switzerland

Received October 25, 2019; Accepted November 5, 2019; Epub February 1, 2020; Published February 15, 2020

Abstract: Mucinous ovarian carcinoma (mEOC) represents a rare subtype of epithelial ovarian cancer, accounting for 3-4% of all ovarian carcinomas. The rarity of this tumor type renders both the preclinical and clinical research compelling. Very few preclinical *in vitro* and *in vivo* models exist. We here report the molecular, metabolic and pharmacological characterization of two patient derived xenografts (PDXs) from mEOC, recently obtained in our laboratory. These PDXs maintain the histological and molecular characteristics of the patient's tumors they derived from, including a wild type *TP53*. Gene expression analysis and metabolomics profile suggest that they differ from high grade serous/endometrioid ovarian carcinoma PDXs. The pharmacological characterization was undertaken testing the *in vivo* antitumor activity of both cytotoxic agents (cisplatin, paclitaxel, yondelis, oxaliplatin and 5-fluorouracile) and targeted agents (bevacizumab and lapatinib). These newly established mucinous PDXs do recapitulate mEOC and will be of value in the preclinical development of possible new therapeutic strategies for this tumor type.

Keywords: Patient-derived xenografts, mucinous ovarian cancer, chemotherapy

Introduction

Mucinous ovarian carcinoma (mEOC) represents a rare subtype of epithelial ovarian cancer, accounting for 3-4% of all ovarian carcinomas [1-4]. These tumors represent a distinct entity in the plethora of epithelial ovarian carcinomas with different epidemiologic and genetic risk factors, somatic alterations, clinical presentation and therapeutic response [5]. As recently reported, they represent "both a diagnostic and therapeutic conundrum for clinical oncologists" [6]. The histological diagnosis of mEOC can be very challenging, and a correct differential diagnosis from metastases originating from the colon rectum is mandatory as standard clinical therapeutic protocol are tailored to the primary organ sites [7].

Most of mEOCs are diagnosed at early stage, have a low histologic grade and are generally associated with a good prognosis [8]. Those cases presenting at late stage have a poor prognosis for their resistance to the platinum-taxane doublet, the gold standard front-line therapy in ovarian cancer. In fact, it has been reported that overall survival (OS) is lower for women with advanced mEOC than women with other advanced non-mucinous histological types (hazard ratio 2.81; 95% CI 2.47-3.21) [9-11]. This is probably due to its lower therapeutic response to first-line based platinum therapy, reported to be 13-60% versus 64-87% in serous ovarian carcinoma patients [3, 6].

At a genetic level, mEOC is rarely associated with *BRCA1/BRCA2* mutations [12, 13], while

an activation of the RAS/MEK pathway is quite common [12] with *RAS* mutations reported in 65% of the cases [12, 13]. *TP53* mutations and *HER2* amplification have been shown to be acquired later in tumor development [12, 14, 15].

The rarity of this tumor type renders both the preclinical and clinical research compelling. Very few preclinical *in vitro* and *in vivo* models exist [16, 17]. Specifically, only immortalized cell lines from established tumor samples and at the best to our knowledge no PDXs and no transgenic mice giving rise to mEOC have been reported. Recently, organoids obtained from mucinous ovarian tumor samples have been established, but their contribution to the biology and therapy of mEOC is still lacking [18]. The availability of robust preclinical models will certainly help not only in a better understanding of the biological behaviour and the therapeutic response of this tumor type, but also to find new active tailored treatments. In the last twenty years, our laboratory has been involved in the establishment of ovarian carcinoma xenobank transplanting fresh patient' tumor samples both orthotopically and/or subcutaneously in immune-compromised animals [19, 20]. We here report the biological, molecular and pharmacological characterization of two mEOC PDXs we have available in our xenobank.

Materials and methods

Specimen collection and clinical data

Clinical specimens (primary ovarian tumors) were obtained from patients undergoing surgery for ovarian tumor by laparotomy at San Gerardo Hospital in Monza (Italy). Tumor specimens were engrafted in nude mice within 24 hr, as already reported [19]. The study protocol for tissue collection and clinical information was approved by the institutional review boards and patients provided written informed consent authorizing the collection and use of the tissue for study purposes.

Animals

Female NCr-nu/nu mice obtained from Envigo Laboratories (The Netherlands) were used when six to eight weeks old. Mice were maintained under specific pathogen-free conditions, housed in isolated vented cages, and handled using aseptic procedures. The Istituto di Ricerche Farmacologiche Mario Negri IRCCS, adheres to the principles set out in the following laws, regulations, and policies governing the care and use of laboratory animals: Italian Governing Law (D. lg 26/2014; authorization no.19/2008-A issued 6 March 2008 by the Ministry of Health); Mario Negri Institutional Regulations and Policies providing internal authorization for persons conducting animal experiments (Quality Management System Certificate: UNI EN ISO 9001:2008, reg. no. 6121); the National Institute of Health (NIH) Guide for the Care and Use of Laboratory Animals (2011 edition) and EU directive and guidelines (European Economic Community [EEC] Council Directive 2010/63/UE) [21].

Histopathological analysis

The morphology of patient's tumor tissues was compared with their corresponding xenografts using paraffin-embedded sections and standard protocols as detailed in [22].

Drugs and treatments

Paclitaxel (Indena s.p.a., Milan, Italy) was dissolved in 50% CremophorEL (Sigma-Aldrich) and 50% ethanol and further diluted with saline before use. Cisplatin (CDDP, Sigma-Aldrich, Milan, Italy) and bevacizumab (Roche, Milan, Italy) were dissolved in 0.9% NaCl. Oxaliplatin (Sigma-Aldrich, Milan, Italy), 5-fluorouracile (5FU) (Sigma-Aldrich, Milan, Italy) were dissolved in sterile H_2O. Yondelis, kindly supplied by PharmaMar, S.A. (Colmenar Viejo, Spain), was dissolved in water and further diluted in saline immediately before use. Lapatinib (Sigma-Aldrich, Milan, Italy) was dissolved in methylcellulose 0.5% and 0.1% Tween-80®.

After subcutaneous transplantation of PDXs, mice were randomized to treatment at approximately 150 mg of tumor weight (8-10 mice per group). Mice were monitored twice a week; tumor growth was measured with a Vernier caliper, and tumor weight (mg = mm^3) calculated as follows: (length [mm] × $width^2$ [mm^2])/2 and body weight was registered as indirect measure of drug toxicity. Treatment efficacy was expressed as best tumor growth inhibition [%T/C = (median weight of treated tumors/ median weight of control tumors) × 100].

Animals were euthanized when primary tumor volume exceeded 15% of body weight. Drug activity was interpreted as follows: subcutaneous tumors were considered resistant with T/C ≥ 50%, responsive with 10% < T/C < 50% and very responsive with T/C ≤ 10%, according to published criteria [23].

Genome-wide gene expression

Microarray data analysis deposited into the NCBI (National Center for Biotechnical Information) database Gene Expression Omnibus (GEO accession no.GSE56920) of patient and xenograft samples have already been reported [19]. Deregulated genes in mucinous PDXs (PDX#164 and PDX#182) as compared to seven high grade serous/endometrioid PDXs were analyzed for enrichment in cancer hallmarks using the web-based tool of the Molecular Signaling Database (MsigDB, http://software.broadinstitute.org/gsea/msigdb) filtering for a false discovery rate (FDR) < 0.05.

Genome-wide DNA profiling

Copy number variation data were obtained using the HumanCytoSNP-12 (Illumina, San Diego, CA, USA), following the manufacturer's protocol. Raw data were processed as previously described [24].

Metabolomic profiling of tumor tissue

Metabolite extraction: For each xenograft, 20-50 mg of each tumor was homogenized using an Ultra Turex with 10 µl/mg of extraction solvent (85:15 MeOH/H_2O). The homogenized sample were stored at -80°C for 20 minute and subsequently centrifuged for 15 minute at 13000 × g. Supernatants were collected and used for targeted and untargeted metabolomics analysis.

Untargeted metabolomics analysis (FIA-QTOF-MS/MS): FIA-QTOF-MS/MS analysis was performed on an Agilent 1290 infinity Series coupled to an Agilent 6550 iFunnel Q-TOF mass spectrometer as reported in Ricci et al. *(manuscript accepted, Therapeutic advances in Molecular Oncology).*

Targeted metabolomics analysis: A targeted quantitative approach using a combined direct flow injection and liquid chromatography (LC) tandem mass spectrometry (MS/MS) assay (AbsoluteIDQ 180 kit, Biocrates, Innsbruck, Austria) was applied as previously published [25].

Statistical analysis

One-way ANOVA followed by Mann-Whitney-Wilcoxon test (JMP Pro13) was used to select the metabolites whose abundance was statistically significant altered between high grade serous and mucinous PDXs. Hierarchical clustering was done using the MeV module (http://mev.tm4.org).

Results

PDX establishment

Two mucinous ovarian carcinomas were established from freshly transplanted mucinous ovarian cancer samples transplanted in immune-deficient mice (see Material and Methods) (MNHOC164 and MNHOC182, from here in PDX#164 and PDX#182). Supplementary Table 1 shows patient's characteristics. Patient #164 was a 56 year woman who was diagnosed with an ovarian mass of malignant origin, who underwent six cycles of neo-adjuvant chemotherapy (carboplatin-paclitaxel) obtaining a stable disease, followed by cyto-reductive surgery (from which we obtained the fresh sample) and histological diagnosis of ovary mucinous adenocarcinoma of intestinal type. On the contrary, patient #182 was a 44 year old woman diagnosed with a Stage I ovary mucinous adenocarcinoma of intestinal type, grade 1 with borderline areas, who underwent pelvic surgery with complete debulking of the tumor mass, point at which we obtained the tumor sample to be inoculated in nude mice. This patient was not treated with any adjuvant chemotherapy, but unfortunately, she relapsed after 42 months.

Lag times for the patient derived xenografts (PDX) to appear were about 30 and 60 days for PDX#164 and PDX#182, respectively. No modification of the tumor lag times was observed with subsequent passages and the tumor take was 100% for PDX#164 and 60% for PDX#182. The pathological diagnosis of both PDXs was ovarian mucinous adenocarcinoma of intestinal type. In addition, as shown in **Figure 1**, both PDXs resembled the original

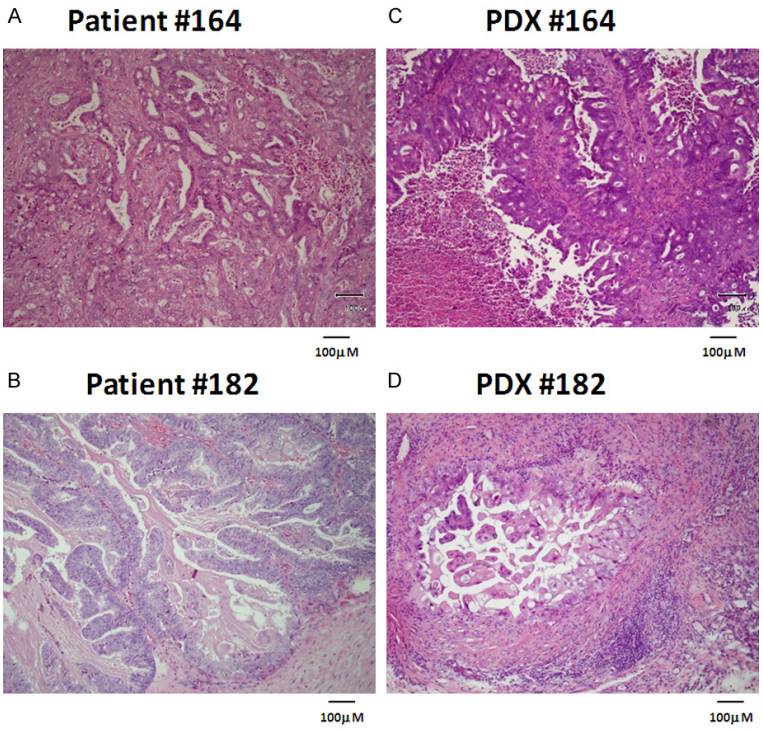

Figure 1. Mucinous ovarian PDX#164 and PDX#182 (C, D) are representative of the primary tumors of origin (A, B). Immunohistochemical analysis of patient's tumors and the corresponding PDXs.

tumors as the morphology and tissue architecture were similarly preserved. Scanty positivity to cytokeratin 7 and CA125 was similar in patient original tumor and the corresponding PDX in the case of PDX#164; while no materials was available for patient #182, PDX#182 was positive for both CA125 and cytokeratin pool; both PDXs were Ki67 positive (Supplementary Figure 1).

From fresh tumor samples, we tried to obtain stem cell enriched cultures as already reported [22]; however, for cells derived from patients #164 and #182 cultured in low adherence condition, we could obtained spheroids that could be maintained for three and four passages respectively, but eventually exhausted their capacity to sustain spheroid formation. Again, up to now even using different cell culture conditions we were unsuccessful in obtaining either spheroids and primary cultures from both PDX samples.

Molecular and metabolic characterization

As already reported, both PDXs were *TP53, RAS, BRAF, PIK3CA* wild type and have an amplification of *ERBB2*, resembling the original tumors [19]. We performed genome wide DNA profiling (Supplementary Table 2) and similar profiles were observed in PDX#182 as compared to the original patient's tumor, while PDX#164 revealed an increased number of heterozygous and homozygous deletions as compared to the corresponding original tumor (Supplementary Table 2) In particular, PDX#164 had acquired different homozygous losses, including the ones affecting the *CDKN2A* and *CDKN2B* (9p21) (heterozygous in the primary) and *DCC* (18q21) loci (Supplementary Figure 2).

We have already reported a high correlation between the expression profile of PDX and the corresponding primary tumors, suggesting that no major molecular drift has occurred in the *in vivo* establishment of the mucinous ovarian PDXs [20]. We then compared the expression profile of high grade-serous and -endometrioid PDXs (number of samples 7) and the two mucinous PDXs we had available. Supplementary Table 3 shows the pathways differentially down and upregulated; among the most upregulated, there is the one involved in metastases, while among the down regulated ones there are the TNFA signalling via NFkB and the apoptosis signalling via caspase activation (Supplementary Table 3).

We investigated the metabolomics profile of PDX#164 and PDX#182 using an integrative mass spectrometry-based approach in which we combined targeted (T) and untargeted (UT) strategies, to compare the metabolic profiles between the two high grade serous PDXs of our xenobank (PDX#124, PDX#239) and the two mucinous PDXs. We observed similar central cellular metabolic profile (glycolysis, TCA cycle) between the high-grade and mucinous PDXs (**Figure 2A**). Interestingly, PDX#164 displayed striking differences in the abundance of lysophosphatidylcholines, phosphatidylcholines and sphingomyelins species compared to PDX#182 and high-grade PDXs (**Figure 2B** and Supplementary Table 4).

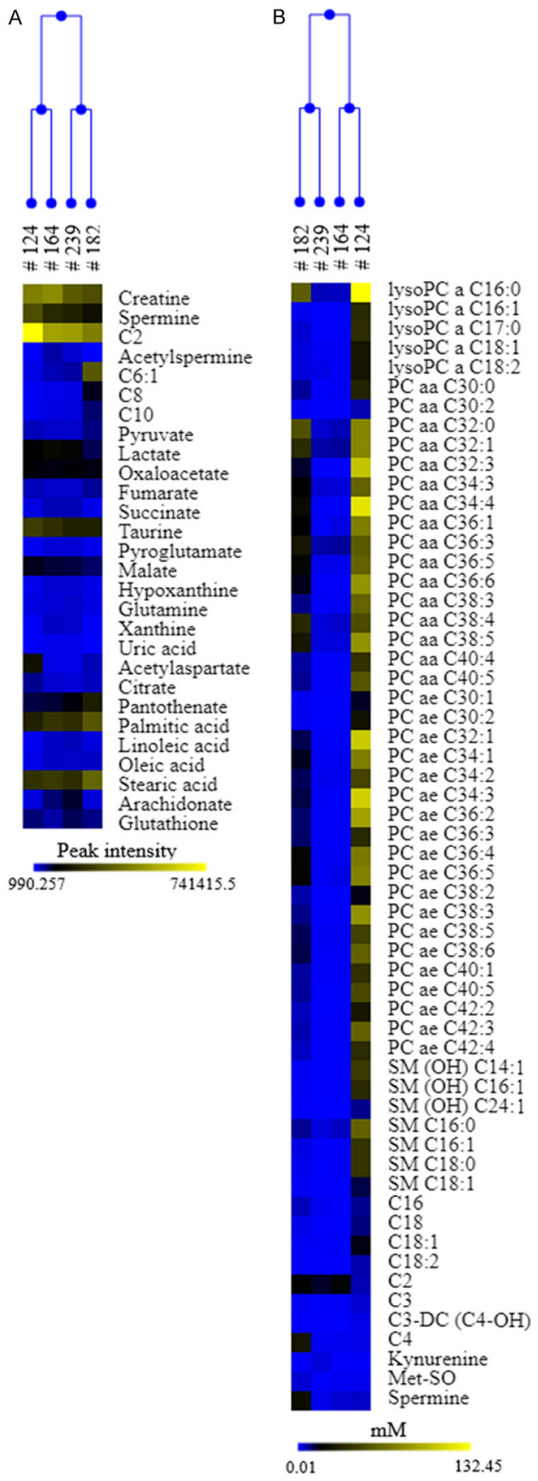

Figure 2. Metabolic comparison between mucinous and serous PDXs. Heat map and hierarchical clustering of the deregulated metabolites (A) untargeted (peak intensity); (B) targeted (mM) in high grade serous (#124, #239) and mucinous (#164, #182) PDXs. Each row represents a metabolite, each column the average metabolite intensity/concentration (three biological replicates) for each PDXs. Blue colour indicates lower metabolite level, yellow higher ones.

Pharmacological characterization

We pharmacologically profiled these mEOC-PDXs testing initially drugs used in first line, i.e. cisplatin and paclitaxel. As depicted in **Figure 3A**, paclitaxel and cisplatin, at the schedules used, were found active in PDX#164, with low T/C values, read out of effective tumor growth inhibition (**Table 1**); however, no tumor regressions were observed during therapy and all the treated tumors regrew. Yondelis, a DNA damaging agents, was inactive in this tumor model. We also tested bevacizumab, an antiangiogenic drug approved for maintenance setting in ovarian cancer, found to be moderately active; on the contrary, oxaliplatin and 5FU were completely inactive (**Figure 3C**). When the same compounds were tested in the PDX#182 model, this xenograft poorly responded to cisplatin and yondelis, while partially responded to paclitaxel (**Figure 3B**; **Table 1**). PDX#182 scarcely responded to oxaliplatin and 5FU, while again a partial response to bevacizumab could be observed (**Figure 3D**). We tested lapatinib, a small molecule inhibitor of the ERBB2 receptor, and no antitumor activity was observed, despite the already reported ERBB2 gene amplification in this PDX [19] and the use of an active schedule in other animal models [26].

Discussion

Preclinical models of mEOC are limited, reflecting the fact that this tumor type is quite rare [3, 6]. As for all rare diseases, the lack of preclinical validated model greatly delays the understanding of their pathogenesis and consequently the development of possible new therapeutic strategies.

We here report the molecular and pharmacological characterization of two mucinous PDXs recently obtained in our laboratory: PDX#164 and PDX#182, both obtained from fresh tumor samples of patients diagnosed with mEOC. While PDX#164 derived from a Stage IV tumor, PDX#182 derived from a Stage I tumor; however patient #182 relapsed after 42 months, suggesting that the original tumor has some aggressive features responsible also for its tumorigenicity in immune-compromised mice. Histological and gene expression profile as compared to the original patient tumors highlight a high degree of similarity. CGH analysis suggest that PDX#182 was very similar to the

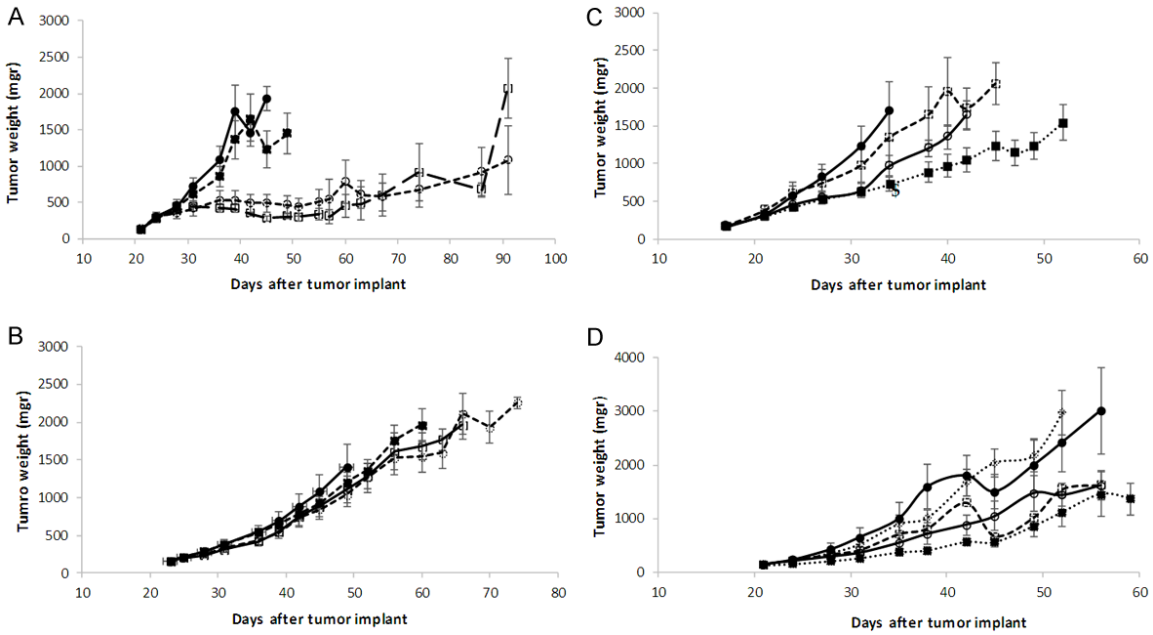

Figure 3. Drugs antitumor activity in mucinous ovarian cancer PDXs. Tumor bearing nude mice #164 (A) and #182 (B) were treated or not (control mice) -●-; with DDP (cisplatin, i.v., 5 mk/Kg, q7dx3) - -○- -; with PTX (paclitaxel, i.v., 20 mg/Kg, q7dx3) -□-; and yondelis (i.v., 0, 15 mg/Kg, q7dx3) - -■- -. Tumor bearing nude mice #164 (C) and #182 (D) were treated or not (control mice) -●-; with oxaliplatin (i.v., 10 mk/Kg, q7dx3) - - □ -, with 5FU (i.v., 75 mg/Kg in #164, 50 mg/Kg in #182, q7dx3) --○--; with bevacizumab (i.p., 5 mg/Kg, q7dx4) ···■···, and with lapatinib (p.o., 100 mg/Kg, 5dx4) ···○···. The graphs represent the mean ± SE of each group (8 mices per group).

Table 1. Antitumor activity in PDX#164 and PDX#182

Drugs	PDX#164	PDX#182
DDP	30.4 (36)	50 (56)
Paclitaxel	24 (36)	39.2 (63)
Yondelis	78.4 (36)	55.9 (46)
Bevacizumab	42.7 (34)	26.1 (38)
Oxaliplatin	79.3 (34)	51.2 (38)
5FU	52.1 (31)	44.9 (38)
Lapatinib	-	63.7 (38)

The best T/C% values (day) are reported for every type of treatment.

tumor of origin, while higher number of deletions could be observed in PDX#164 as regards corresponding primary tumor. Loss of heterozygous and homozygous deletions in 9pand 9p21.3 have been reported to be early events in mucinous ovarian cancers, occurring in 60% of benign tumors and with higher percentages in borderlines tumors, suggesting that the silencing of $p16^{INK4A}$, ARF and $p15^{INK4B}$, protein coded by genes located in 9p21.3, offers a selective growth advantage [27]. The homozygous deletion we observed in PDX#164 as compared to the corresponding patients sample would confirm this hypothesis. Both patient and tumor samples harbor a wild type *TP53* [19]. While *TP53* has been reported to be usually mutated in high grade serous ovarian carcinoma [28], it is less frequently mutated in mEOC [6, 12, 29]. The fact that we were able to obtain PDXs from wild type *TP53* fresh tumor samples and that these could be successfully maintained through multiple rounds of serial transplantations, suggest that mutation in *TP53* is not a tumor driver for this ovarian histotype. *RAS* mutations, frequently reported in mEOC, characterized our PDXs. The transcriptomic profile of mucinous PDXs resemble the origin patient' samples [19]. When their gene expression profiles were compared to the ones of 7 high grade serous/endometrial PDXs, a downregulation of the apoptosis signalling via caspase activation, supporting the fact that mucinous carcinomas are much less responsive to chemotherapy [6].

The metabolomics study, performed with the idea to characterize this rare tumor type and compared it with high grade PDXs, suggests a comparable central cellular metabolic asset

among these histotypes. We found a divergence in the lipid content (phosphatidylcholines and sphingomyelin species) in PDX#164, that could be due to the induction of specific phospholipase C (PC-PLC) and/or *de novo* sphingolipid biosynthetic pathways already reported in some tumors [30, 31].

We finally tested the antitumor activity of different drugs. PDX#164 was quite sensitive to both platinum and paclitaxel and these data seem to contrast with the fact that patient had a stable disease after neo-adjuvant chemotherapy. These apparently contrasting results could have different reasons: i) the experimental setting is completely different. The patient had a quite diffuse disease (stage IV), while mice have been randomized when tumor masses were little (150 mgr); ii) the clinical efficacy endpoint used (stable disease) is different from the *in vivo* anticancer activity parameter we used. The disease stabilization observed could be similar to the tumor growth inhibition observed with both cisplatin and paclitaxel, as no treated mice underwent tumor regressions. Indeed, in the majority of high grade serous ovarian carcinoma, cisplatin and paclitaxel induced a clear regression in PDXs and response in patients [19]. On the contrary, PDX#182 was completely resistant to these drugs and this better mimics the mEOC therapeutic response to ovarian gold standard therapy. The histological similarity with metastatic mucinous colon rectal cancer has suggested that mEOC could indeed be much more sensitive to drugs currently used for colon cancer (antimetabolite and oxaliplatin) than to the platinum based/paclitaxel chemotherapy [32, 33]. We tested in both xenografts, the antitumor activity of oxaliplatin and 5FU and again no activity were observed. These data parallel the preliminary data of Gynecologic Oncology Group trial (GOG) 241, an international phase 3 study, in which metastatic mucinous ovarian cancer patients were randomly assigned to receive paclitaxel and carboplatin (control group) or the combination of capecitabine and oxaliplatin [34]. Due to the slow accrual, the trial was closed; however, results on 50 patients suggest that there were no difference in progression free survival and response rates (very low) between the two arms. The failing of the randomized GOG241trial has underlined the difficulty to carry out randomized clinical trials in mEOC and has led to the suggestion to randomize these patients in trials of non-gynecological mucinous tumors [4].

We here report the molecular, metabolic and pharmacological characterization of two PDXs from ovarian mucinous carcinomas. These PDXs represent the original tumors from which they derived. The molecular and metabolic data suggest that these tumors are quite different from the more common high-grade serous/endometrioid ovarian carcinomas. In addition, the pharmacological profile partially reflects what observed in the clinical setting. We are aware of the fact that the presented data rely on only two PDXs; however, considering the rarity of this tumor types, we think that these models represent mEOC and they will be of value in the preclinical development of possible new therapeutic strategies for this tumor type.

Acknowledgements

This research was funded by the Italian Association for Cancer Research (AIRC), grant number IG 19797 to GD. The generous contributions of AIRC (The Italian Association for Cancer Research) is grateful acknowledged.

Disclosure of conflict of interest

None.

Address correspondence to: Giovannna Damia, Laboratory of Molecular Pharmacology, Istituto di Ricerche Farmacologiche Mario Negri IRCCS, Milan 20156, Italy. E-mail: giovanna.damia@marionegri.it

References

[1] Seidman JD, Horkayne-Szakaly I, Haiba M, Boice CR, Kurman RJ and Ronnett BM. The histologic type and stage distribution of ovarian carcinomas of surface epithelial origin. Int J Gynecol Pathol 2004; 23: 41-4.

[2] Heinzelmann-Schwarz VA, Gardiner-Garden M, Henshall SM, Scurry JP, Scolyer RA, Smith AN, Bali A, Vanden Bergh P, Baron-Hay S, Scott C, Fink D, Hacker NF, Sutherland RL and O'Brien PM. A distinct molecular profile associated with mucinous epithelial ovarian cancer. Br J Cancer 2006; 94: 904-13.

[3] Ricci F, Affatato R, Carrassa L and Damia G. Recent insights into mucinous ovarian carcinoma. Int J Mol Sci 2018; 19.

[4] Leary AF, Quinn M, Fujiwara K, Coleman RL, Kohn E, Sugiyama T, Glasspool R, Ray-Coquard

I, Colombo N, Bacon M, Zeimet A, Westermann A, Gomez-Garcia E, Provencher D, Welch S, Small W, Millan D, Okamoto A, Stuart G and Ochiai K; Participants of the Fifth Ovarian Cancer Consensus Conference. Fifth Ovarian Cancer Consensus Conference of the Gynecologic Cancer InterGroup (GCIG): clinical trial design for rare ovarian tumours. Ann Oncol 2017; 28: 718-726.

[5] Perren TJ. Mucinous epithelial ovarian carcinoma. Ann Oncol 2016; 27 Suppl 1: i53-i57.

[6] Morice P, Gouy S and Leary A. Mucinous ovarian carcinoma. N Engl J Med 2019; 380: 1256-1266.

[7] Simons M, Bolhuis T, De Haan AF, Bruggink AH, Bulten J, Massuger LF and Nagtegaal ID. A novel algorithm for better distinction of primary mucinous ovarian carcinomas and mucinous carcinomas metastatic to the ovary. Virchows Arch 2019; 474: 289-296.

[8] Cobb LP and Gershenson DM. Treatment of rare epithelial ovarian tumors. Hematol Oncol Clin North Am 2018; 32: 1011-1024.

[9] Hess V, A'Hern R, Nasiri N, King DM, Blake PR, Barton DP, Shepherd JH, Ind T, Bridges J, Harrington K, Kaye SB and Gore ME. Mucinous epithelial ovarian cancer: a separate entity requiring specific treatment. J Clin Oncol 2004; 22: 1040-4.

[10] Winter WE 3rd, Maxwell GL, Tian C, Carlson JW, Ozols RF, Rose PG, Markman M, Armstrong DK, Muggia F and McGuire WP; Gynecologic Oncology Group Study. Prognostic factors for stage III epithelial ovarian cancer: a gynecologic oncology group study. J Clin Oncol 2007; 25: 3621-7.

[11] Firat Cuylan Z, Karabuk E, Oz M, Turan AT, Meydanli MM, Taskin S, Sari ME, Sahin H, Ulukent SC, Akbayir O, Gungorduk K, Gungor T, Kose MF and Ayhan A. Comparison of stage III mucinous and serous ovarian cancer: a case-control study. J Ovarian Res 2018; 11: 91.

[12] Ryland GL, Hunter SM, Doyle MA, Caramia F, Li J, Rowley SM, Christie M, Allan PE, Stephens AN and Bowtell DD; Australian Ovarian Cancer Study Group; Campbell IG and Gorringe KL. Mutational landscape of mucinous ovarian carcinoma and its neoplastic precursors. Genome Med 2015; 7: 87.

[13] Mackenzie R, Kommoss S, Winterhoff BJ, Kipp BR, Garcia JJ, Voss J, Halling K, Karnezis A, Senz J, Yang W, Prigge ES, Reuschenbach M, Doeberitz MV, Gilks BC, Huntsman DG, Bakkum-Gamez J, McAlpine JN and Anglesio MS. Targeted deep sequencing of mucinous ovarian tumors reveals multiple overlapping RAS-pathway activating mutations in borderline and cancerous neoplasms. BMC Cancer 2015; 15: 415.

[14] Chang KL, Lee MY, Chao WR and Han CP. The status of Her2 amplification and Kras mutations in mucinous ovarian carcinoma. Hum Genomics 2016; 10: 40.

[15] Mueller JJ, Schlappe BA, Kumar R, Olvera N, Dao F, Abu-Rustum N, Aghajanian C, DeLair D, Hussein YR, Soslow RA, Levine DA and Weigelt B. Massively parallel sequencing analysis of mucinous ovarian carcinomas: genomic profiling and differential diagnoses. Gynecol Oncol 2018; 150: 127-135.

[16] Hisamatsu T, McGuire M, Wu SY, Rupaimoole R, Pradeep S, Bayraktar E, Noh K, Hu W, Hansen JM, Lyons Y, Gharpure KM, Nagaraja AS, Mangala LS, Mitamura T, Rodriguez-Aguayo C, Eun YG, Rose J, Bartholomeusz G, Ivan C, Lee JS, Matsuo K, Frumovitz M, Wong KK, Lopez-Berestein G and Sood AK. PRKRA/PACT expression promotes chemoresistance of mucinous ovarian cancer. Mol Cancer Ther 2019; 18: 162-172.

[17] Takata A, Terauchi M, Hiramitsu S, Uno M, Wakana K and Kubota T. Dkk-3 induces apoptosis through mitochondrial and Fas death receptor pathways in human mucinous ovarian cancer cells. Int J Gynecol Cancer 2015; 25: 372-9.

[18] Kopper O, de Witte CJ, Lõhmussaar K, Valle-Inclan JE, Hami N, Kester L, Balgobind AV, Korving J, Proost N, Begthel H, van Wijk LM, Revilla SA, Theeuwsen R, van de Ven M, van Roosmalen MJ, Ponsioen B, Ho VWH, Neel BG, Bosse T, Gaarenstroom KN, Vrieling H, Vreeswijk MPG, van Diest PJ, Witteveen PO, Jonges T, Bos JL, van Oudenaarden A, Zweemer RP, Snippert HJG, Kloosterman WP and Clevers H. An organoid platform for ovarian cancer captures intra- and interpatient heterogeneity. Nat Med 2019; 25: 838-849.

[19] Ricci F, Bizzaro F, Cesca M, Guffanti F, Ganzinelli M, Decio A, Ghilardi C, Perego P, Fruscio R, Buda A, Milani R, Ostano P, Chiorino G, Bani MR, Damia G and Giavazzi R. Patient-derived ovarian tumor xenografts recapitulate human clinicopathology and genetic alterations. Cancer Res 2014; 74: 6980-90.

[20] Ricci F, Fratelli M, Guffanti F, Porcu L, Spriano F, Dell'Anna T, Fruscio R and Damia G. Patient-derived ovarian cancer xenografts re-growing after a cisplatinum treatment are less responsive to a second drug re-challenge: a new experimental setting to study response to therapy. Oncotarget 2017; 8: 7441-7451.

[21] Workman P, Aboagye EO, Balkwill F, Balmain A, Bruder G, Chaplin DJ, Double JA, Everitt J, Farningham DA, Glennie MJ, Kelland LR, Robinson V, Stratford IJ, Tozer GM, Watson S, Wedge SR and Eccles SA; Committee of the National Cancer Research Institute. Guidelines for the wel-

fare and use of animals in cancer research. Br J Cancer 2010; 102: 1555-77.
[22] Ricci F, Bernasconi S, Perego P, Ganzinelli M, Russo G, Bono F, Mangioni C, Fruscio R, Signorelli M, Broggini M and Damia G. Ovarian carcinoma tumor-initiating cells have a mesenchymal phenotype. Cell Cycle 2012; 11: 1966-76.
[23] Massazza G, Tomasoni A, Lucchini V, Allavena P, Erba E, Colombo N, Mantovani A, D'Incalci M, Mangioni C and Giavazzi R. Intraperitoneal and subcutaneous xenografts of human ovarian carcinoma in nude mice and their potential in experimental therapy. Int J Cancer 1989; 44: 494-500.
[24] Rinaldi A, Kwee I, Young KH, Zucca E, Gaidano G, Forconi F and Bertoni F. Genome-wide high resolution DNA profiling of hairy cell leukaemia. Br J Haematol 2013; 162: 566-9.
[25] Brunelli L, Caiola E, Marabese M, Broggini M and Pastorelli R. Comparative metabolomics profiling of isogenic KRAS wild type and mutant NSCLC cells in vitro and in vivo. Sci Rep 2016; 6: 28398.
[26] Zhang WJ, Li Y, Wei MN, Chen Y, Qiu JG, Jiang QW, Yang Y, Zheng DW, Qin WM, Huang JR, Wang K, Zhang WJ, Wang YJ, Yang DH, Chen ZS and Shi Z. Synergistic antitumor activity of regorafenib and lapatinib in preclinical models of human colorectal cancer. Cancer Lett 2017; 386: 100-109.
[27] Hunter SM, Gorringe KL, Christie M, Rowley SM and Bowtell DD; Australian Ovarian Cancer Study Group, Campbell IG. Pre-invasive ovarian mucinous tumors are characterized by CDKN2A and RAS pathway aberrations. Clin Cancer Res 2012; 18: 5267-77.
[28] Cancer Genome Atlas Research Network. Integrated genomic analyses of ovarian carcinoma. Nature 2011; 474: 609-15.
[29] Rechsteiner M, Zimmermann AK, Wild PJ, Caduff R, von Teichman A, Fink D, Moch H and Noske A. TP53 mutations are common in all subtypes of epithelial ovarian cancer and occur concomitantly with KRAS mutations in the mucinous type. Exp Mol Pathol 2013; 95: 235-41.
[30] Iorio E, Caramujo MJ, Cecchetti S, Spadaro F, Carpinelli G, Canese R and Podo F. Key Players in choline metabolic reprograming in triple-negative breast cancer. Front Oncol 2016; 6: 205.
[31] Ogretmen B. Sphingolipid metabolism in cancer signalling and therapy. Nat Rev Cancer 2018; 18: 33-50.
[32] Sato S, Itamochi H, Kigawa J, Oishi T, Shimada M, Sato S, Naniwa J, Uegaki K, Nonaka M and Terakawa N. Combination chemotherapy of oxaliplatin and 5-fluorouracil may be an effective regimen for mucinous adenocarcinoma of the ovary: a potential treatment strategy. Cancer Sci 2009; 100: 546-51.
[33] Xu W, Rush J, Rickett K and Coward JI. Mucinous ovarian cancer: a therapeutic review. Crit Rev Oncol Hematol 2016; 102: 26-36.
[34] Gore ME, Hackshaw A, Brady WE, Penson RT, Zaino RJ, McCluggage WG, et al. Multicentre trial of carboplatin/paclitaxel versus oxaliplatin/capecitabine, each with/without bevacizumab, as first line chemotherapy for patients with mucinous epithelial ovarian cancer (mEOC). J Clin Oncol 2015; 33 Suppl: 5528-5528.

Supplementary Table 1. Characteristics of patients #164 and #182 from which PDXs derived from

Xeno ID	Age	Stage	Hystotype	Grade	Residual tumor	Chemotheapy	Schedule	No of cycles	PFS
164	56	IV	Mucinous carcinoma	2	na	neo-adjuvant	CBDCA/Tax	6	5
182	44	IC	Mucinous carcinoma	1	NED	-	-	-	42

NED non evidence of disesase. na not available.

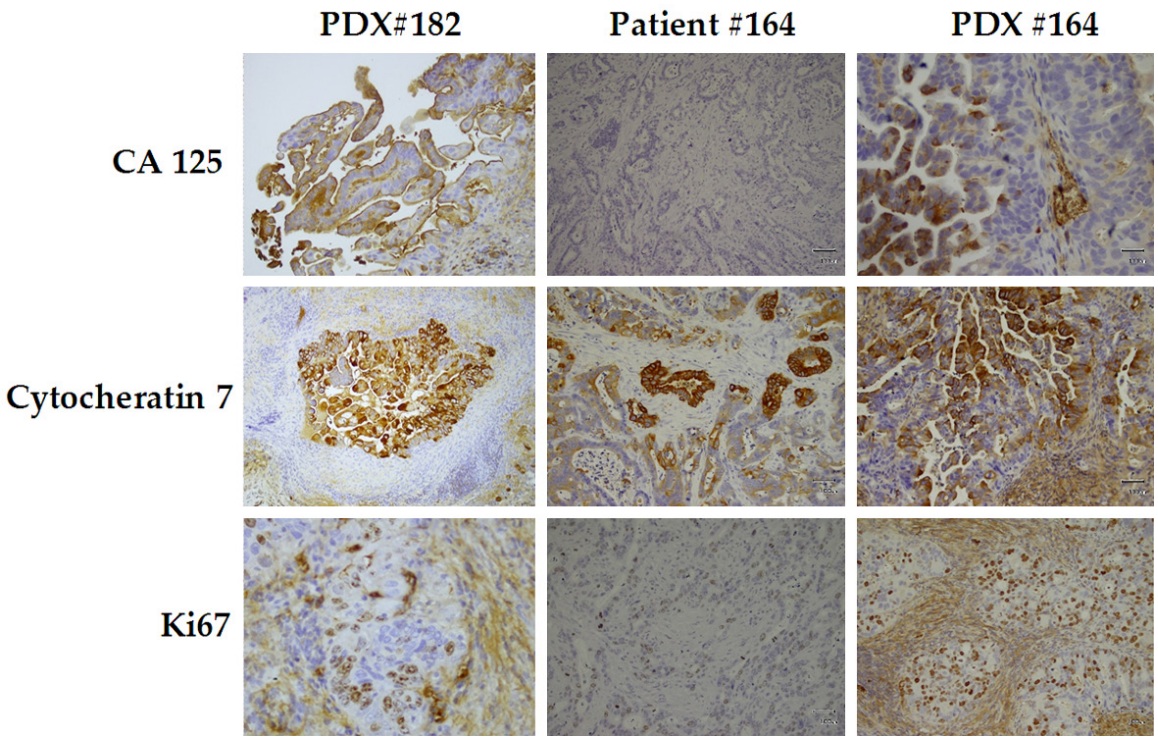

Supplementary Figure 1. Immunohistochemical analysis on PDX and patient's #164, and on PDX's #182.

Supplementary Table 2. CGH analysis. The table reports the alteration observed in #164 and #182, both in patients and PDXs samples

ID	chrom	loc.start	loc.end	type	seg.mean	ID	chrom	loc.start	loc.end	type	seg.mean
						PDX#164	1	47226827	71195538	LOSS	-0.23383612
						PDX#164	1	90373067	103454621	LOSS	-0.200775
						PDX#164	1	220627747	222012950	LOSS	-0.1729463
patient #164	2	51951101	58264394	LOSS	-0.13212025	PDX#164	2	51751984	58192905	LOSS	-0.2538235
patient #164	2	88591175	98329197	LOSS	-0.14849373	PDX#164	2	88355735	90247720	LOSS	-0.50372969
						PDX#164	2	91812834	98303915	LOSS	-0.17649264
						PDX#164	2	115872796	116841792	LOSS	-0.49634463
						PDX#164	2	159512538	162169631	LOSS	-0.30143563
						PDX#164	3	24186625	93737580	LOSS	-0.20101206
patient #164	4	90421700	187866343	LOSS	-0.11807837	PDX#164	4	20714719	22435993	LOSS	-0.37643872
						PDX#164	4	34595824	40598634	LOSS	-0.21799649
						PDX#164	4	90958046	187866343	LOSS	-0.23232617
patient #164	5	43704556	152621660	LOSS	-0.12453422	PDX#164	5	28286502	28601552	LOSS	-0.5111838
						PDX#164	5	49952847	135758057	LOSS	-0.23260105
						PDX#164	5	135764923	136003152	HDEL	-2.87880778
						PDX#164	5	140588373	153616916	LOSS	-0.26152751
patient #164	6	58738122	61929807	HDEL	-0.83391937	PDX#164	6	1374277	28521316	LOSS	-0.20510848
						PDX#164	6	70137886	85181754	LOSS	-0.21755622
						PDX#164	6	85205713	85518398	HDEL	-2.47892978
						PDX#164	6	85521035	101562017	LOSS	-0.23053892
						PDX#164	6	101568294	102417713	HDEL	-2.16270399
						PDX#164	6	102423940	110447643	LOSS	-0.23646079
						PDX#164	6	110532805	118091629	GAIN	0.120967829
						PDX#164	6	118103840	123172683	LOSS	-0.21727506
						PDX#164	6	123183020	170898549	GAIN	0.101023285
patient #164	7	55848790	66689729	LOSS	-0.13485114	PDX#164	7	34777714	37958289	LOSS	-0.25117862
patient #164	7	102828569	104289858	LOSS	-0.18103569	PDX#164	7	40054784	42283788	LOSS	-0.30869191
patient #164	8	70761794	72742860	LOSS	-0.16135322	PDX#164	8	176818	43646413	LOSS	-0.17136785
patient #164	8	144626533	144899538	LOSS	-0.35671155	PDX#164	8	70222636	72871111	LOSS	-0.20269474
						PDX#164	8	72872544	77560474	GAIN	0.125503941
						PDX#164	8	77575477	79654145	LOSS	-0.23937531
						PDX#164	8	79686236	80214806	HDEL	-1.80037814
patient #164	9	20793269	29112301	LOSS	-0.22625262	PDX#164	9	17444478	21150650	LOSS	-0.15240683
						PDX#164	9	21157373	23092415	HDEL	-2.60981006

						PDX#164	9	23121911	29052442	LOSS	-0.27108901
patient #164	10	135708	135430043	LOSS	-0.11131817	PDX#164	10	135708	23708636	LOSS	-0.22796377
						PDX#164	10	23755800	25705149	HDEL	-2.09178179
						PDX#164	10	25740053	56018508	LOSS	-0.22554604
						PDX#164	10	56076004	57628056	HDEL	-2.5021768
						PDX#164	10	57667668	64602767	LOSS	-0.32362268
						PDX#164	10	64615451	66612353	LOSS	-0.31556414
						PDX#164	10	66702282	68680367	HDEL	-1.90789248
						PDX#164	10	68687179	109115199	LOSS	-0.22824603
						PDX#164	10	109173829	110688807	HDEL	-1.88233379
						PDX#164	10	110697497	135430043	LOSS	-0.20661974
patient #164	11	21632174	26521821	LOSS	-0.13287578	PDX#164	11	21894814	23783338	LOSS	-0.26411404
patient #164	11	48647107	50467850	LOSS	-0.20076055	PDX#164	11	47983477	67408791	LOSS	-0.19684138
patient #164	11	50474459	51366191	LOSS	-0.56786599	PDX#164	11	67414492	74360030	GAIN	0.105256015
patient #164	11	51372036	64147083	LOSS	-0.11666955	PDX#164	11	74366331	124190137	LOSS	-0.10683956
patient #164	11	77069746	124227543	LOSS	-0.10617829	PDX#164	11	124227543	134944006	GAIN	0.139078978
patient #164	12	7520771	9813414	LOSS	-0.31594017	PDX#164	12	6128984	8023943	LOSS	-0.23968702
						PDX#164	12	8029351	8274082	HDEL	-2.31281488
						PDX#164	12	8280908	8509503	HDEL	-0.65846985
						PDX#164	12	8609795	9428169	HDEL	-2.41970498
						PDX#164	12	9451761	9816429	LOSS	-0.32804057
						PDX#164	12	41723032	42942234	LOSS	-0.22340097
						PDX#164	12	46670589	49512017	LOSS	-0.20045613
						PDX#164	12	74690292	78768977	LOSS	-0.18942913
patient #164	13	66357912	115106996	GAIN	0.107197262	PDX#164	13	57464113	66324372	LOSS	-0.21301909
patient #164	14	106681665	107023065	AMPL	1.127471562	PDX#164	14	50563262	51195365	LOSS	-0.36233976
						PDX#164	14	106681665	107023065	AMPL	0.780347864
patient #164	15	20161372	20577494	LOSS	-0.28658878	PDX#164	15	20161372	26746446	LOSS	-0.1201309
						PDX#164	15	26752373	26872259	HDEL	-1.0675029
patient #164	16	46820464	48132847	LOSS	-0.14603658	PDX#164	16	72911406	74171216	LOSS	-0.24258104
						PDX#164	16	74183855	88302760	GAIN	0.114546239
patient #164	17	44163925	44799962	LOSS	-0.49388819						
patient #164	18	47709926	52717564	LOSS	-0.1310454	PDX#164	18	28109801	48111941	LOSS	-0.17619072
						PDX#164	18	48114756	50039676	HDEL	-2.47616174
						PDX#164	18	50043368	52483586	LOSS	-0.27688464
						PDX#164	18	65009233	69958047	LOSS	-0.20462023

						PDX#164	19	19683350	20397555	LOSS	-0.41962018
						PDX#164	21	10734842	17242234	LOSS	-0.42742183
						PDX#164	21	20415950	25158258	LOSS	-0.12592933
						PDX#164	21	25165525	27414889	LOSS	-0.51966215
						PDX#164	22	16079545	51169045	LOSS	-0.11285165
patient #164	23	7335191	7517325	AMPL	0.917457097	PDX#164	23	126729969	127403730	HDEL	-0.69614929
ID	chrom	loc.start	loc.end	type	seg.mean	ID	chrom	loc.start	loc.end	type	seg.mean
patient #82	6	58738122	62230131	LOSS	-0.33187307						
patient #82	7	61905009	64284502	LOSS	-0.23511491						
patient #82	8	144670950	144899538	LOSS	-0.46173432						
patient #82	9	10291546	12247973	LOSS	-0.22640716						
patient #82	11	21712019	28237516	LOSS	-0.12125467	PDX#182	11	50345592	51366191	LOSS	-0.37653636
patient #82	11	48647107	50460079	LOSS	-0.17863142						
patient #82	11	50467850	51366191	HDEL	-0.76198416						
patient #82	14	106681665	106997898	AMPL	1.48395907	PDX#182	14	106391073	107023065	GAIN	0.566176383
patient #82	14	107023065	107282437	GAIN	0.124723335	PDX#182	14	107032603	107282437	LOSS	-0.14755029
patient #82	19	23534190	24368053	LOSS	-0.18175417						
patient #82	19	24368534	28379648	LOSS	-0.46060025						
patient #82	22	18901004	19016663	GAIN	0.364652091						
patient #82	23	7335191	7528738	AMPL	1.203133776						
patient #82	23	7537276	8115453	GAIN	0.11469615						

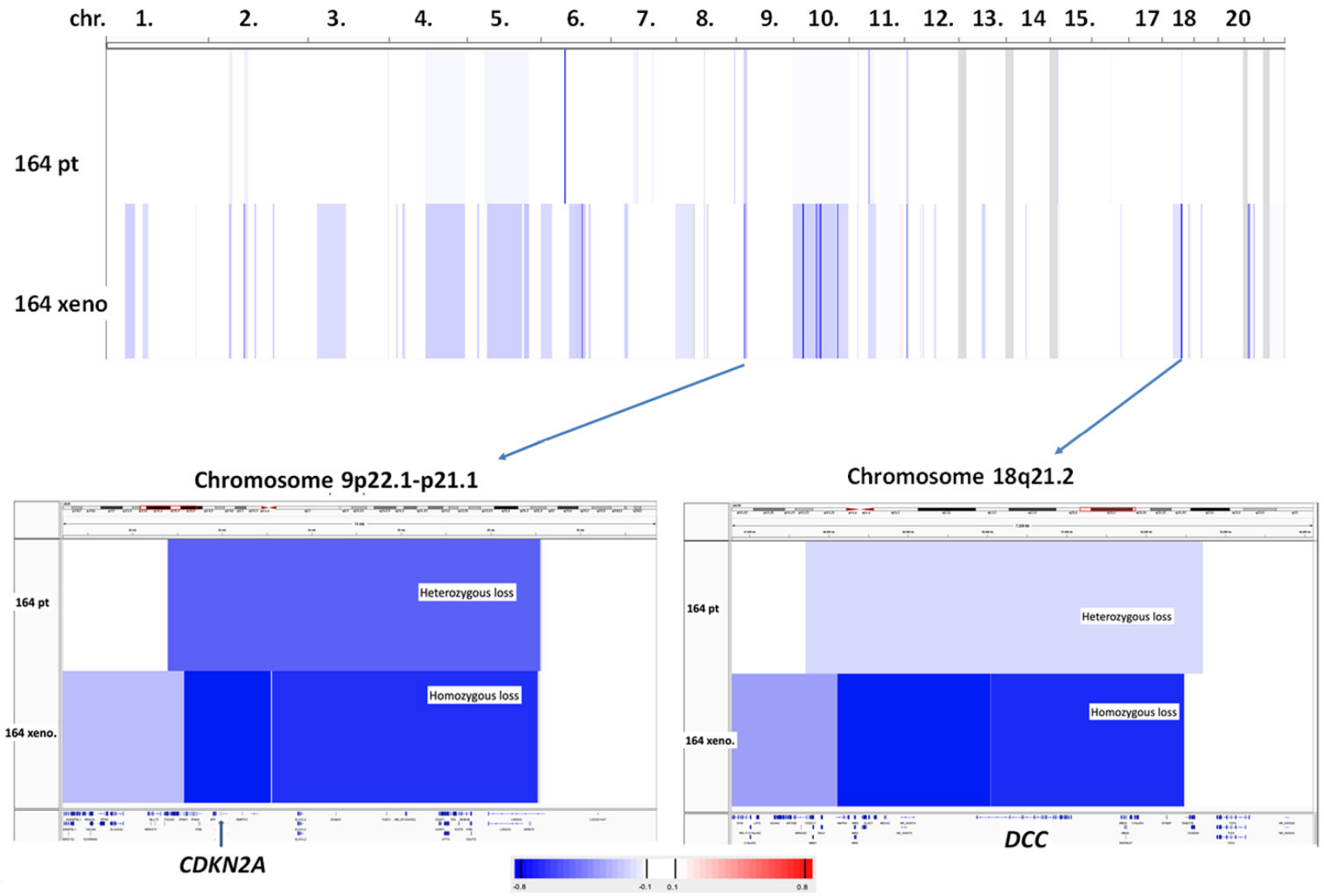

Supplementary Figure 2. Copy number variation analysis in patients #164 and its corresponding PDX. Upper plot represents the heatmap of copy number changes across the genome. Lower plots focuses on CDKN2A and DCC genes loci. In both panels: white, normal copy number; blue, DNA loss; red, DNA gain.

Supplementary Table 3. Pawthway enrichment analysis in mucinous PDXs as compared to hiugh grade serous/endometriod PDXs

Gene Set Name	# Genes in Gene Set (K)	Description	# Genes in Overlap (k)	k/K	*p*-value	FDR q-value
JAEGER_METASTASIS_UP	44	Genes up-regulated in metastases from malignant melanoma compared to the primary tumors.	3	0.0682	3.61E-06	4.76E-02
SATO_SILENCED_BY_METHYLATION_IN_PANCREATIC_CANCER_1	419	Genes up-regulated in the pancreatic cancer cell lines (AsPC1, Hs766T, MiaPaCa2, Panc1) but not in the non-neoplastic cells (HPDE) by decitabine (5-aza-2'-deoxycytidine) [PubChem=451668].	5	0.0119	8.60E-06	4.76E-02
GSE2706_LPS_VS_R848_AND_LPS_8H_STIM_DC_DN	200	Genes down-regulated in comparison of dendritic cells (DC) stimulated with LPS (TLR4 agonist) at 8 h versus DCs stimulated with LPS (TLR4 agonist) and R848 for 8 h.	4	0.02	9.99E-06	4.76E-02
Gene Set Name	# Genes in Gene Set (K)	Description	# Genes in Overlap (k)	k/K	*p*-value	FDR q-value
HALLMARK_TNFA_SIGNALING_VIA_NFKB	200	Genes regulated by NF-kB in response to TNF [GeneID=7124].	9	0.045	7.47E-09	3.74E-07
HALLMARK_APICAL_JUNCTION	200	Genes encoding components of apical junction complex.	8	0.04	1.30E-07	3.25E-06
HALLMARK_IL2_STAT5_SIGNALING	200	Genes up-regulated by STAT5 in response to IL2 stimulation.	7	0.035	1.98E-06	3.30E-05
HALLMARK_EPITHELIAL_MESENCHYMAL_TRANSITION	200	Genes defining epithelial-mesenchymal transition, as in wound healing, fibrosis and metastasis.	6	0.03	2.62E-05	3.27E-04
HALLMARK_APOPTOSIS	161	Genes mediating programmed cell death (apoptosis) by activation of caspases.	5	0.0311	1.07E-04	1.07E-03
HALLMARK_ESTROGEN_RESPONSE_LATE	200	Genes defining late response to estrogen.	5	0.025	2.94E-04	1.83E-03
HALLMARK_MITOTIC_SPINDLE	200	Genes important for mitotic spindle assembly.	5	0.025	2.94E-04	1.83E-03
HALLMARK_XENOBIOTIC_METABOLISM	200	Genes encoding proteins involved in processing of drugs and other xenobiotics.	5	0.025	2.94E-04	1.83E-03
HALLMARK_UV_RESPONSE_DN	144	Genes down-regulated in response to ultraviolet (UV) radiation.	4	0.0278	8.19E-04	4.55E-03
HALLMARK_UV_RESPONSE_UP	158	Genes up-regulated in response to ultraviolet (UV) radiation.	4	0.0253	1.15E-03	5.77E-03
HALLMARK_IL6_JAK_STAT3_SIGNALING	87	Genes up-regulated by IL6 [GeneID=3569] via STAT3 [GeneID=6774], e.g., during acute phase response.	3	0.0345	2.06E-03	9.36E-03
HALLMARK_ESTROGEN_RESPONSE_EARLY	200	Genes defining early response to estrogen.	4	0.02	2.73E-03	9.73E-03
HALLMARK_INFLAMMATORY_RESPONSE	200	Genes defining inflammatory response.	4	0.02	2.73E-03	9.73E-03
HALLMARK_KRAS_SIGNALING_UP	200	Genes up-regulated by KRAS activation.	4	0.02	2.73E-03	9.73E-03
HALLMARK_WNT_BETA_CATENIN_SIGNALING	42	Genes up-regulated by activation of WNT signaling through accumulation of beta catenin CTNNB1.	2	0.0476	6.54E-03	2.18E-02

Supplementary Table 4. Metabolomic analysis (untargeted and targeted) on high-grade serous/endometriod (#124, #239) and mucinous ovarian carcinoma (#182, #164)

Metabolites	Fold Change	Peak intensity										Adduct	Mw_mean
		High grade serous						Mucinous					
		#124			#239			#182		#164			
Creatine	1.09	228833.2	305577.9	320288.7	432260.1	389198.2	406463.6	473933.4	407565	460742.7	174265.3	M+H	132.0769
Spermine	-1.14	96460.75	146801.7	157175.1	337359.9	242466.4	279307.7	137152.4	250907.4	247377	103961.5	M+H	203.2232
Acetylcarnitine	-1.16	366178.3	381830.2	468221.6	739855.9	703406.4	741415.5	665684.9	326560.6	292845.6	668086.6	M+H	204.1242
N1-Acetylspermine	17.63	0	0	0	2535.41	3609.909	2483.7	6745.919	58172.18	32011.23	4509.496	M+H	245.2334
Hexanoylcarnitine	-5.31	265414.4	324020.5	345591.5	9672.969	7472.402	13976.67	40215.29	12546.24	12971.31	55460.85	M+H	260.1859
Octanoylcarnitine	-4.02	70392.93	85899.29	88564.12	3057.612	2721.775	5525.541	13938.99	5289.471	4558.743	18646.87	M+H	288.2169
Decanoylcarnitine	-2.40	44855.78	53548.33	59501.01	4322.136	4347.306	7166.844	11620.86	11302.45	10650.26	14628.94	M+H	316.2481
Stearoylcarnitine	1.03	104048.1	120308.5	201365.9	28442.79	24712.26	47338.2	51165.41	121550.9	173809.9	13164.46	M+H	428.3728
pyruvate	-1.89	43953.1	47688.57	46379.98	27194.73	28971.02	21595.23	26191.38	12454.61	10085.34	27353.59	M-H	87.00887
lactic acid	1.34	72003.43	60500.05	60391.76	107347.1	90665.49	86154.4	123149.3	100769.9	105540.9	95471.23	M-H	89.02453
Oxalacetic acid	1.01	85551.33	90015.6	83150.14	90978.8	90982.21	88475.51	89708.87	85394.51	87838.23	92181.96	M-H	112.9856
fumarate	-1.61	36537.71	39288.87	38162.33	26739.47	31083.41	22524.44	25259.82	15673.96	14512.53	25142.9	M-H	115.0036
succinate	2.89	7132.301	8456.018	7403.189	14638.82	9608.096	8801.011	21042.56	33688.93	35584.64	17810.19	M-H	117.0192
Taurine	-1.10	177192	181394	161201	270453.4	215748.9	249176.1	223930.2	191422.2	160597.8	185014.9	M-H	124.0073
Pyroglutamic acid	2.33	7714.318	8293.904	7240.291	5707.378	6178.577	5632.256	16589.44	15084.66	10292.03	21377	M-H	128.0352
malate	1.04	52873.76	54826.86	58612.18	75048.6	99263.5	71718.49	71847.6	73192.88	76268.8	64056.33	M-H	133.0141
Hypoxanthine	2.11	9752.633	8634.266	9584.405	7834.029	6384.18	7489.89	9065.039	26797.52	21050.41	12823.1	M-H	135.0303
Glutamine	1.54	15068.73	11684.82	5935.058	10868.63	12511.1	12059.12	24047.5	6931.186	26322.21	12532.41	M-H	145.0617
Xanthine	5.45	4107.661	2760.118	4793.89	5393.98	2120.585	3778.583	5793.8	38559.95	27783.52	11299.31	M-H	151.0259
Uric acid	4.58	1880.298	991.4921	1724.652	2868.161	1359.515	1443.211	10060.69	5663.07	5063.052	10543.61	M-H	167.0209
N-Acetyl-L-aspartic acid	-8.01	26361.08	25842.79	26555.23	87379.41	180810.1	127591.2	18244.34	2374.491	1857.783	17033.33	M-H	174.0407
Citric acid	-1.92	23440.87	23287.9	27555.34	28437.22	48794.96	43898.11	25582.46	12331.08	12129.58	17880.49	M-H	191.0195
Pantothenic acid	-1.44	182209.1	163429.7	149892	82019.9	62769.01	61679.26	108630.2	37952.23	48938.42	129097.6	M-H	218.1031
Palmitic acid	-1.14	424097.1	263380.1	236264.9	130630	217812.3	177980	259444.7	182471.7	218265.3	187504.3	M-H	255.2329
Linoleic acid	2.65	14271.92	9028.383	12708.97	4896.332	7453.251	5095.058	15929.72	27061.11	27342.97	24104.9	M-H	279.2324
Oleic acid	1.41	35591.02	11022.09	17483.79	5406.544	11896.4	9392.697	14371.9	28910.29	29055.8	12784.84	M-H	281.248
Stearic acid	-1.27	454076.9	298429.4	277048.6	152648.2	274069.5	223892.4	312610.4	157925.3	257256.1	154177.8	M-H	283.2642
Arachidonic acid	4.58	16950.42	10499.97	15985.38	12365.39	16992.79	10647.9	33696.31	69307.82	47879.95	103768.4	M-H	303.2323
Glutathione	-1.02	35733.33	50362.12	48598.28	49568.08	51453.06	50315.18	30078.42	35096.96	95817.24	25226.16	M-H	306.0757
		μM											
Sample Identification		High grade serous						Mucinous					
		#124			#239			#182		#164			
lysoPC a C16:0	3.50	36.7	67.2	46.6	4.546667	3.546667	3.116667	3.796667	2.456667	105.55	159.35		
lysoPC a C16:1	51.54	0.860667	1.249	0.806667	0.090667	0.104667	0.091	0.085	0.076667	27.65	39.45		
lysoPC a C17:0	18.64	1.53	3.406667	1.768667	0.125	0.101333	0.093667	0.086	0.066333	30.3	38.35		

lysoPC a C18:1	14.01	2.62	2.01	1.626667	0.711	0.58	0.624	0.541333	0.379	22.9	24.25
lysoPC a C18:2	10.12	2.68	2.263333	1.52	0.824	0.469	0.438667	1.288333	0.906333	23.65	22.75
PC aa C30:0	5.09	6.823333	5.343333	6.013333	0.392333	0.611	0.485	0.234667	0.109667	27.05	33.3
PC aa C30:2	6.75	0.782	0.953667	0.819	0.015333	0.022	0.018333	0.007333	0.004667	3.665	5.2
PC aa C32:0	2.70	61.8	44.13333	58.6	4.043333	4.683333	3.333333	2.666667	1.293	104	48.05
PC aa C32:1	2.77	56.73333	33.86667	34.2	3.156667	6.993333	4.613333	4.876667	1.305	90.2	62
PC aa C32:3	13.47	11.24333	10.61333	12.49	0.139	0.204667	0.149333	0.141333	0.034333	137.5	72.5
PC aa C34:3	7.58	18.7	14.33333	13.38	1.35	2.623333	1.610333	2.49	0.674333	55.55	64.7
PC aa C34:4	6.51	20.6	17.6	18.83333	0.310667	0.542667	0.4	0.411	0.115667	108	132.5
PC aa C36:1	6.60	19.23333	13.53333	14.26667	1.297667	1.786667	1.408667	0.361	0.271333	67.8	77.65
PC aa C36:3	2.08	40.66667	26.56667	21.96667	3.31	7.326667	3.846667	4.72	1.574667	47.55	64.1
PC aa C36:5	4.64	22.03333	16.63333	14.93333	0.584333	1.141	0.726667	1.122333	0.263667	83.95	35
PC aa C36:6	8.21	12.33	11.28667	13.91667	0.078667	0.118	0.097667	0.092	0.024333	106.9	58.9
PC aa C38:3	10.29	8.176667	6.323333	6.873333	0.386667	0.671333	0.380667	0.268	0.123333	77.9	43.45
PC aa C38:4	1.54	54.26667	35.8	28.56667	2.252	4.08	2.025	2.174	0.839333	42.25	56.05
PC aa C38:5	3.58	39.5	25.5	23.36667	1.277667	2.64	1.4	1.879333	0.450667	120	44.5
PC aa C40:4	10.71	6.563333	5.223333	5.25	0.109667	0.118333	0.085333	0.064667	0.025	9.1	64.15
PC aa C40:5	12.57	7.333333	5.676667	5.96	0.106667	0.170667	0.101	0.096	0.025667	70.8	35.85
PC ae C30:1	22.55	0.770333	0.707333	0.854667	0.039333	0.057333	0.041333	0.037667	0.016667	5.35	18.56
PC ae C30:2	23.05	0.949333	1.071333	1.044	0.012667	0.014667	0.012	0.01	0.004667	16	28.45
PC ae C32:1	16.14	10.33667	8.636667	10.61	0.375667	0.688333	0.495333	0.289	0.121333	149.8	65.7
PC ae C34:1	6.37	15.96667	12.04667	12.73333	0.621667	1.09	0.670667	0.546667	0.202	66.25	78.5
PC ae C34:2	5.14	11.33333	9.24	9.086667	0.444333	1.097667	0.575667	0.792667	0.338333	75.85	15.45
PC ae C34:3	15.85	10.34	9.026667	11.58333	0.186333	0.468667	0.261667	0.385667	0.278	107.8	112.5
PC ae C36:2	12.09	9.06	7.586667	8.26	0.348667	0.655667	0.373333	0.442	0.286333	137	41.95
PC ae C36:3	9.38	9.313333	7.886667	8.68	0.179667	0.394	0.278	0.335667	0.144667	36.5	29.4
PC ae C36:4	5.67	23.46667	16.36667	16.5	0.437	0.738667	0.392667	0.648667	0.217667	99.35	41.75
PC ae C36:5	6.19	17.8	15.03333	15.96667	0.528333	1.727333	1.036333	0.473667	0.278	81.25	67.5
PC ae C38:2	12.17	5.243333	4.106667	5.403333	0.044667	0.071667	0.041667	0.047	0.031333	6.75	19.4
PC ae C38:3	10.97	7.266667	6.036667	7.18	0.092333	0.149667	0.085667	0.074	0.032	113.5	48.15
PC ae C38:5	8.24	13.1	9.163333	9.283333	0.427	0.848667	0.55	0.52	0.140667	36.85	50.25
PC ae C38:6	7.22	11.93333	9.663333	10.23333	0.155333	0.428	0.261	0.251667	0.068	87.5	30.75
PC ae C40:1	7.11	7.006667	5.543333	5.226667	0.245	0.499667	0.297	0.437	0.146	47.45	23.95
PC ae C40:5	8.90	5.763333	5.36	5.84	0.062333	0.084667	0.053667	0.051333	0.022667	57.45	37.5
PC ae C42:2	11.18	4.29	3.503333	3.763333	0.034333	0.069667	0.05	0.030333	0.014	16.55	32.43
PC ae C42:3	15.72	4.923333	4.21	4.406667	0.088333	0.143333	0.089667	0.091	0.041333	90.15	27.8
PC ae C42:4	12.99	3.503333	3.223333	3.163333	0.005	0.007	0.003	0.003667	0.005	24.6	43.55
sugars	51.35	588.3333	498	270.3333	102.4333	122.8667	37.5	116.1	27.4	18503.5	23667.5
Kynurenine	2.86	0.421333	0.410667	0.518333	0.573667	0.251667	0.184667	2.026667	2.353333	0.4725	0.3715
Met-SO	-2.96	4.933333	3.23	1.81	1.209	0.802	0.585667	0.314667	0.281667	0.4825	1.265
Spermine	-3.80	2.264667	4.296667	35.3	3.203333	2.492333	2.59	1.09	1.15	2	4.195

t4-OH-Pro	2.24	7.41	6.963333	6.523333	3.293333	3.91	3.683333	4.7	4.743333	14.65	21.45
Taurine	1.04	813.3333	922	876.3333	190	196	201	204.6667	210.6667	704.5	831
Cit	3.96	12.66667	11.8	9.963333	2.44	1.53	1.553333	7.076667	3.773333	26.05	64.25
Gly	1.30	486.6667	445.6667	382.6667	396	443	427.6667	271.3333	348.6667	611	960
His	1.14	46.93333	40.73333	39.8	22.63333	18.57667	17.3	16.6	15.16667	29.7	66.45
Met	-1.34	54.66667	48.2	41.63333	16.43333	11.74333	10.6	8.556667	9.19	25.15	41.8
Pro	1.05	157.3333	126.6667	122.7667	130.3333	104.1	126	54.76667	56	145	256
SM (OH) C14:1	98.23	0.562667	0.613667	0.558333	0.067333	0.105333	0.055667	0.048	0.039	50.5	32.05
SM (OH) C16:1	63.88	0.62	0.603	0.534	0.076	0.121333	0.078333	0.026333	0.022333	45.3	21.8
SM (OH) C24:1	31.55	0.261667	0.295	0.233333	0.005333	0.006333	0.006333	0.005667	0.001333	0.6565	11.96
SM C16:0	6.68	6.753333	6.693333	4.963333	2.443333	3.916667	2.833333	1.886667	1.171667	78.55	39.3
SM C16:1	30.35	2.073333	1.716667	1.385	0.192	0.333667	0.207333	0.341	0.221	31.55	44.4
SM C18:0	26.28	1.108333	1.186667	0.877667	0.389667	0.561	0.450667	0.159667	0.084333	29.95	46.1
SM C18:1	21.61	1.03	0.702333	0.547667	0.077667	0.165333	0.104	0.062	0.041	5.11	15.05
C16	2.17	2.803333	2.766667	4.493333	0.219	0.177667	0.231	0.695333	0.302	6.03	6.145
C18	6.50	0.842667	0.650667	1.627667	0.118667	0.158	0.182667	0.195667	0.072333	6.53	7.64
C18:1	22.52	0.418667	0.428333	0.758333	0.098667	0.071667	0.115667	0.460333	0.176	12.5	13.25
C18:2	9.95	0.361	0.516667	0.608333	0.057333	0.042	0.059	0.312	0.207	4.375	4.88
C2	-1.94	11.89	12.5	15.9	16.66667	14.22	15.33333	11.73333	12.9	4.32	4.07
C3	2.85	0.744667	0.662	0.691	0.486333	0.525667	0.453	0.274667	0.558667	2.66	2.405
C3-DC (C4-OH)	3.28	0.339333	0.334	0.356333	0.212667	0.179333	0.160667	0.180667	0.204	1.37	1.24
C4	-11.68	29.1	23.23333	23.03333	1.154	0.848	1.066667	0.676333	0.653333	1.52	1.405